ARTICLE IN PRESS

Journal of Computational Physics xxx (2011) xxx–xxx

Contents lists available at ScienceDirect

Journal of Computational Physics

journal homepage: www.elsevier.com/locate/jcp

Factored singularities and high-order Lax–Friedrichs sweeping schemes for point-source traveltimes and amplitudes

Songting Luo, Jianliang Qian *,[1]

Department of Mathematics, Michigan State University, East Lansing, MI 48824, USA

ARTICLE INFO

Article history:
Received 11 August 2010
Received in revised form 20 January 2011
Accepted 26 February 2011
Available online xxxx

Keywords:
Hamilton–Jacobi equations
Lax–Friedrichs
WENO schemes
Fast sweeping methods
Factored singularity
Eikonal solver

ABSTRACT

In the high frequency regime, the geometrical-optics approximation for the Helmholtz equation with a point source results in an Eikonal equation for traveltime and a transport equation for amplitude. Because the point-source traveltime field has an upwind singularity at the source point, all formally high-order finite-difference Eikonal solvers exhibit first-order convergence and relatively large errors. In this paper, we propose to first factor out the singularities of traveltimes, takeoff angles, and amplitudes, and then we design high-order Lax–Friedrichs sweeping schemes for point-source traveltimes, takeoff angles, and amplitudes. Numerical examples are presented to demonstrate the performance of our new method.

© 2011 Elsevier Inc. All rights reserved.

1. Introduction

In the high frequency regime, the geometrical-optics approximation for the Helmholtz equation with a point source results in an Eikonal equation for traveltime and a transport equation for amplitude. Because the point-source traveltime field has an upwind singularity at the source point, all formally high-order finite-difference Eikonal solvers exhibit first-order convergence and relatively large errors. Moreover, the resultant inaccuracy in traveltime prevents reliable computations of takeoff angles and amplitudes. In this paper, we propose to first factor out the singularities of traveltimes, takeoff angles, and amplitudes; based on this factorization, we design high-order Lax–Friedrichs sweeping schemes for point-source traveltimes, takeoff angles, and amplitudes.

Many finite-difference and finite-element methods have been introduced to solve the Eikonal equation with a point-source condition. In the vast literature, we cite just a few of them to illustrate the point: [27,26,19,20,23,10,16,29,25,9,17,18,7,12]. The traveltime field is mostly smooth, suggesting that high-order finite-difference methods should be effective. The use of upwind schemes in all of the cited methods confines the errors to singularities which develop away from the source point. However, the source point itself is an upwind singularity. Thus most of the published high-order Eikonal solvers for point-source conditions have to initialize the traveltime field analytically near the source by imposing a grid-independent region of constant velocity near the source; see [22,28,21]. This approach has two essential drawbacks: (1) the velocity may not be homogeneous near the source, and (2) the size of the region of analytic computations must be set by the user and bears no direct relation to the grid parameters. In principle, highly accurate ray-tracing methods may be used to alleviate the first difficulty, but the second remains: it introduces an arbitrary parameter into the use of Eikonal solvers. Although the fixed local

* Corresponding author.
E-mail addresses: luos@math.msu.edu (S. Luo), qian@math.msu.edu (J. Qian).
[1] Qian is supported by NSF 0810104 and NSF 0830161.

0021-9991/$ - see front matter © 2011 Elsevier Inc. All rights reserved.
doi:10.1016/j.jcp.2011.02.043

Please cite this article in press as: S. Luo, J. Qian, Factored singularities and high-order Lax–Friedrichs sweeping schemes for point-source traveltimes and amplitudes, J. Comput. Phys. (2011), doi:10.1016/j.jcp.2011.02.043

grid refinement method proposed in [10] compensates for the loss of accuracy near the source point, it still has an adhoc parameter to be chosen by the user. The adaptive grid refinement method proposed in [16] overcomes these drawbacks successfully, but it incurs a heavy burden in numerical implementation.

To overcome the above difficulties efficiently without any adhoc parameters, we observe that near the source the singularities in traveltime, takeoff angle, and amplitude in inhomogeneous media can be well-captured by those singularities in homogeneous media. Furthermore, inspired by the first-order fast sweeping method for the factored Eikonal equation as in [5], we propose to factor out the singularities explicitly in either multiplicative or additive manner; based on the resulting factorization we design high-order Lax–Friedrichs sweeping schemes for solving factored Eikonal and transport equations. With high-order accurate traveltimes and amplitudes at our disposal, we construct asymptotic wavefields and make comparison with direct solutions of the Helmholtz equation.

The outline of the paper is as follows. In Section 2, we summarize the fundamental equations that we are going to solve. In Section 3, we present the factorizations on the traveltime, takeoff angle and out-of-plane curvature. In Section 4, we present a third-order weighted essentially non-oscillatory (WENO) based Lax–Friedrichs scheme to solve the factored equations. In Section 5, extensive numerical examples are presented to illustrate the performance of the new methods; we also use computed traveltimes and amplitudes to construct the asymptotic Green function and compare the resulting Green function with that obtained by a finite-difference direct solution of the Helmholtz equation. We conclude the paper with some remarks.

2. Fundamental equations

For a source (x_0,z_0) in an isotropic solid, the least traveltime $\tau(x,z)$ is the viscosity solution of an Eikonal equation [13,3],

$$|\nabla\tau| = s(x,z) \tag{1}$$

with the initial condition

$$\lim_{(x,z)\to(x_0,z_0)}\left(\frac{\tau(x,z)}{\sqrt{(x-x_0)^2+(z-z_0)^2}}-\frac{1}{v(x,z)}\right)=0, \tag{2}$$

where $v = 1/s$ is the velocity.

Based on the traveltime field, one can compute the amplitude field by solving the transport equation [2],

$$\nabla\tau\cdot\nabla A+\frac{1}{2}A\nabla^2\tau=0. \tag{3}$$

Eq. (3) is a first-order advection equation for the amplitude A. In order to get a first-order accurate amplitude field, one needs a third-order accurate traveltime field since the Laplacian of the traveltime field is involved; see a detailed argument in [16].

Denoting ϕ as the takeoff angle of a ray from the source point (x_0,z_0) to a general point (x,z), it is constant along any ray

$$\nabla\tau\cdot\nabla\phi=\frac{\partial\tau}{\partial x}\frac{\partial\phi}{\partial x}+\frac{\partial\tau}{\partial z}\frac{\partial\phi}{\partial z}=0. \tag{4}$$

Since the wavefront normal $\nabla\tau$ is tangential to the ray in an isotropic solid, the gradient $\nabla\phi$ is tangential to the wavefront.

In 2D isotropic media with line sources, the amplitude satisfies the formula ([2,6])

$$A=\frac{v\sqrt{|\nabla\tau\times\nabla\phi|}}{2\sqrt{2\pi}}. \tag{5}$$

For a typical seismic point source, one needs to compensate for the out-of-plane radiation in the 2D line source amplitude formula (5). The 2D amplitude with a point source (2.5-D amplitude) can be computed by

$$A=\frac{\sqrt{v\tau_{yy}|\nabla\tau\times\nabla\phi|}}{4\pi}, \tag{6}$$

where the out-of-plane curvature τ_{yy} satisfies an advection equation [24],

$$\frac{\partial\tau}{\partial x}\frac{\partial\tau_{yy}}{\partial x}+\frac{\partial\tau}{\partial z}\frac{\partial\tau_{yy}}{\partial z}+\tau_{yy}^2=0. \tag{7}$$

If a first-order accurate amplitude field is required, then the gradients $\nabla\tau$ and $\nabla\phi$ involved in the amplitude formulas should be at least first-order accurate. According to Eq. (4), at least second-order accurate derivatives of the traveltime τ are required to get first-order accurate $\nabla\phi$. Therefore, at least third-order accurate traveltime τ is required to get a first-order amplitude field.

The point-source traveltime $\tau(x,z)$ has an upwind singularity at the source (x_0,z_0). Any first-order or high-order finite-difference Eikonal solver can formally have first-order convergence and relatively large errors, because the low accuracy near the source can spread out to the whole space. Therefore, to obtain high accuracy in computing point-source traveltimes one

Please cite this article in press as: S. Luo, J. Qian, Factored singularities and high-order Lax–Friedrichs sweeping schemes for point-source traveltimes and amplitudes, J. Comput. Phys. (2011), doi:10.1016/j.jcp.2011.02.043

has to treat this upwind singularity carefully. One possible approach is the adaptive method proposed in [16], in which the mesh near the source is refined adaptively according to a user-specified threshold in accuracy; as a result, the accuracy loss due to the singularity of the traveltime field near the point source is compensated by adaptive mesh refinement near the source. Another approach to treat this singularity is to explicitly factor out the singularity in traveltime field due to the point source as first proposed in [5], in which the traveltime is factorized into two multiplicative factors, one of which being able to capture the source singularity explicitly. This factorization results in an underlying function that is smooth in a neighborhood of the source and satisfies a factored Eikonal equation; consequently, a first-order fast sweeping scheme yields a fully first-order accurate traveltime field as demonstrated in [5].

In this work, we utilize this factorization idea for the point-source traveltime τ and extend it to the takeoff angle ϕ and out-of-plane curvature τ_{yy}. We decompose ϕ into two additive factors; one of the factors is the takeoff angle corresponding to a constant velocity field, thus it is known analytically. We decompose τ_{yy} into two multiplicative factors; one of the factors is the out-of-plane curvature corresponding to a constant velocity field, thus it is known analytically too. The factorization of ϕ or τ_{yy} results in an underlying function that satisfies a factored advection equation. To solve the factored equations, we will design a third-order Lax–Friedrichs sweeping scheme based on the third-order WENO finite-difference reconstruction.

3. Factored Eikonal and transport equations

We first recall the factored Eikonal equation in [5]. Let us consider a factored decomposition

$$\begin{cases} \tau(x,z) = \tau_0(x,z)u(x,z), \\ s(x,z) = s_0(x,z)\alpha(x,z) \end{cases} \tag{8}$$

and assume that τ_0 satisfies

$$|\nabla\tau_0| = s_0 \tag{9}$$

with the initial condition

$$\lim_{(x,z)\to(x_0,z_0)} \left(\frac{\tau_0(x,z)}{\sqrt{(x-x_0)^2+(z-z_0)^2}} - s_0(x,z) \right) = 0. \tag{10}$$

We choose s_0 as some constant, thus

$$\tau_0 = \frac{\sqrt{(x-x_0)^2+(z-z_0)^2}}{v_0},$$

is the traveltime corresponding to the constant velocity field $v_0 = 1/s_0$.

The function substitution transforms the Eikonal Eq. (1) into the factored Eikonal equation

$$\sqrt{\tau_0^2(u_x^2+u_z^2) + 2\tau_0 u(\tau_{0x}u_x + \tau_{0z}u_z) + u^2 s_0^2} = s. \tag{11}$$

The factor τ_0 captures the source singularity such that the underlying function u is smooth in a neighborhood of the source.

For the constant velocity v_0, the takeoff angle in the homogeneous medium, denoted as ϕ_0, is constant along any ray

$$\nabla\tau_0 \cdot \nabla\phi_0 = 0. \tag{12}$$

Thus substituting the following decomposition

$$\phi(x,z) = \phi_0(x,z) + \psi(x,z), \tag{13}$$

into Eq. (4) and using Eqs. (8) and (12), we get a factored advection equation

$$\nabla\psi \cdot (\nabla\tau_0 u + \tau_0\nabla u) + \tau_0\nabla u \cdot \nabla\phi_0 = 0. \tag{14}$$

Because ϕ_0 is known analytically and captures the local properties of ϕ, the underlying additive factor ψ can be viewed as a small perturbation to ϕ_0 locally at the source.

For the constant velocity v_0, the out-of-plane curvature in the homogeneous medium, denoted as τ_{yy0}, satisfies the following advection equation

$$\frac{\partial\tau_0}{\partial x}\frac{\partial\tau_{yy0}}{\partial x} + \frac{\partial\tau_0}{\partial z}\frac{\partial\tau_{yy0}}{\partial z} + \tau_{yy0}^2 = 0. \tag{15}$$

Substituting the decomposition

$$\tau_{yy}(x,z) = \tau_{yy0}(x,z)c(x,z) \tag{16}$$

Please cite this article in press as: S. Luo, J. Qian, Factored singularities and high-order Lax–Friedrichs sweeping schemes for point-source traveltimes and amplitudes, J. Comput. Phys. (2011), doi:10.1016/j.jcp.2011.02.043

into (7) and using Eqs. (8) and (15), we get another factored advection equation

$$(\tau_{yy0}\tau_0\nabla u + \tau_{yy0}u\nabla\tau_0)\cdot\nabla c + (\tau_0\nabla\tau_{yy0}\cdot\nabla u - \tau_{yy0}^2 u)c + \tau_{yy0}^2 c^2 = 0. \tag{17}$$

Since τ_{yy0} is known analytically and captures the source singularity, the underlying factor c is smooth in a neighborhood of the source.

With the decomposition (8) and (13), we have

$$\begin{cases} \nabla\tau = \tau_0\nabla u + u\nabla\tau_0, \\ \nabla\phi = \nabla\phi_0 + \nabla\psi. \end{cases} \tag{18}$$

In order to get $\nabla\tau$, $\nabla\phi$ and τ_{yy}, we need to compute u, ∇u, ψ, $\nabla\psi$ and c. Thus we need to solve the factored Eikonal Eq. (11) and the factored advection Eqs. (14) and (17). The traveltime τ_0, takeoff angle ϕ_0 and out-of-plane curvature τ_{yy0} corresponding to the constant velocity field v_0 capture the source singularity properly so that the underlying functions u, ψ and c are smooth near the source. Consequently, we need not worry about the upwind singularity at the source when solving the factored Eikonal and advection equations, and it is relatively easy to design high-order schemes for solving (11), (14) and (17) so that we can compute the underlying functions u, ψ and c with high accuracy. Once u, ψ and c are available, we can compute the amplitude with formulas (5) or (6).

4. Third-order accurate Lax–Friedrichs scheme

We present Lax–Friedrichs schemes for the factored Eqs. (11), (14) and (17) on a rectangular mesh Ω^h with grid size h which covers the domain Ω. Let us consider the following generic equation

$$H(x,z,u,u_x,u_z) = f(x,z), \tag{19}$$

where H is a given Hamiltonian.

At a grid point $(i,j) = (x_i,z_j)$ with neighbors

$$N\{i,j\} = \{(x_{i-1},z_j),(x_{i+1},z_j),(x_i,z_{j-1}),(x_i,z_{j+1})\},$$

we approximate H by the following Lax–Friedrichs numerical Hamiltonian [14,8]

$$H^{LF}(x_i,z_j,u_{ij},u_{N\{ij\}}) = H\Big(x_i,z_j,u_{ij},\frac{u_{i+1j}-u_{i-1j}}{2h},\frac{u_{ij+1}-u_{ij-1}}{2h}\Big) - \alpha_x\frac{u_{i+1j}-2u_{ij}+u_{i-1j}}{2h} - \alpha_z\frac{u_{ij+1}-2u_{ij}+u_{ij-1}}{2h}, \tag{20}$$

where α_x and α_z are chosen such that, for fixed (x_i,z_j),

$$\begin{aligned}
&\frac{\partial H^{LF}}{\partial u_{ij}} = \frac{\partial H}{\partial u_{ij}}\Big(x_i,z_j,u_{ij},\frac{u_{i+1j}-u_{i-1j}}{2h},\frac{u_{ij+1}-u_{ij-1}}{2h}\Big) + \frac{\alpha_x+\alpha_z}{h} \geqslant 0,\\
&\frac{\partial H^{LF}}{\partial u_{i+1j}} = \frac{1}{2h}H_1\Big(x_i,z_j,u_{ij},\frac{u_{i+1j}-u_{i-1j}}{2h},\frac{u_{ij+1}-u_{ij-1}}{2h}\Big) - \frac{\alpha_x}{h} \leqslant 0,\\
&\frac{\partial H^{LF}}{\partial u_{i-1j}} = -\frac{1}{2h}H_1\Big(x_i,z_j,u_{ij},\frac{u_{i+1j}-u_{i-1j}}{2h},\frac{u_{ij+1}-u_{ij-1}}{2h}\Big) - \frac{\alpha_x}{h} \leqslant 0,\\
&\frac{\partial H^{LF}}{\partial u_{ij+1}} = \frac{1}{2h}H_2\Big(x_i,z_j,u_{ij},\frac{u_{i+1j}-u_{i-1j}}{2h},\frac{u_{ij+1}-u_{ij-1}}{2h}\Big) - \frac{\alpha_z}{h} \leqslant 0,\\
&\frac{\partial H^{LF}}{\partial u_{ij-1}} = -\frac{1}{2h}H_2\Big(x_i,z_j,u_{ij},\frac{u_{i+1j}-u_{i-1j}}{2h},\frac{u_{ij+1}-u_{ij-1}}{2h}\Big) - \frac{\alpha_z}{h} \leqslant 0.
\end{aligned} \tag{21}$$

H_1 and H_2 denote the derivatives of H with respect to the first and second gradient variable, respectively. For example, we can choose

$$\begin{aligned}
\alpha_x &= \max_{m\leqslant u\leqslant M, A\leqslant p\leqslant B, C\leqslant q\leqslant D}\Big\{\frac{1}{2}|H_1(x,z,u,p,q)| + \Big|\frac{\partial H}{\partial u}(x,z,u,p,q)\Big|\Big\},\\
\alpha_z &= \max_{m\leqslant u\leqslant M, A\leqslant p\leqslant B, C\leqslant q\leqslant D}\Big\{\frac{1}{2}|H_2(x,z,u,p,q)| + \Big|\frac{\partial H}{\partial u}(x,z,u,p,q)\Big|\Big\}.
\end{aligned} \tag{22}$$

The numerical Hamiltonian H^{LF} is monotone for $m \leqslant u_{ij} \leqslant M$, $A \leqslant p \leqslant B$, and $C \leqslant q \leqslant D$ with $p = (u_{i+1j} - u_{i-1j})/2h$ and $q = (u_{ij+1} - u_{ij-1})/2h$. Then we have a first-order Lax–Friedrichs scheme

$$u_{ij}^{new} = \Big(\frac{1}{\alpha_x/h+\alpha_z/h}\Big)\Big[f_{ij} - H\Big(x_i,z_j,u_{ij}^{old},\frac{u_{i+1j}-u_{i-1j}}{2h},\frac{u_{ij+1}-u_{ij-1}}{2h}\Big) + \alpha_x\frac{u_{i+1j}+u_{i-1j}}{2h} + \alpha_z\frac{u_{ij+1}+u_{ij-1}}{2h}\Big]. \tag{23}$$

Please cite this article in press as: S. Luo, J. Qian, Factored singularities and high-order Lax–Friedrichs sweeping schemes for point-source traveltimes and amplitudes, J. Comput. Phys. (2011), doi:10.1016/j.jcp.2011.02.043

To design high-order sweeping schemes, we follow the strategy in [28] to replace $u_{i-1,j}$, $u_{i+1,j}$, $u_{i,j-1}$ and $u_{i,j+1}$ with

$$\begin{aligned} u_{i-1,j} &= u_{i,j} - h(u_x)^-_{i,j}, \quad u_{i+1,j} = u_{i,j} + h(u_x)^+_{i,j}, \\ u_{i,j-1} &= u_{i,j} - h(u_z)^-_{i,j}, \quad u_{i,j+1} = u_{i,j} + h(u_z)^+_{i,j}. \end{aligned} \tag{24}$$

$(u_x)^-_{i,j}$ and $(u_x)^+_{i,j}$ are third-order upwind-biased WENO approximations of u_x;
$(u_z)^-_{i,j}$ and $(u_z)^+_{i,j}$ are third-order upwind-biased WENO approximations of u_z.

That is,

$$(u_x)^-_{i,j} = (1-\omega_-)\left(\frac{u_{i+1,j}-u_{i-1,j}}{2h}\right) + \omega_-\left(\frac{3u_{i,j}-4u_{i-1,j}+u_{i-2,j}}{2h}\right) \tag{25}$$

with

$$\omega_- = \frac{1}{1+2\gamma_-^2}, \quad \gamma_- = \frac{\epsilon + (u_{i,j}-2u_{i-1,j}+u_{i-2,j})^2}{\epsilon + (u_{i+1,j}-2u_{i,j}+u_{i-1,j})^2} \tag{26}$$

and

$$(u_x)^+_{i,j} = (1-\omega_+)\left(\frac{u_{i+1,j}-u_{i-1,j}}{2h}\right) + \omega_+\left(\frac{-3u_{i,j}+4u_{i+1,j}-u_{i+2,j}}{2h}\right) \tag{27}$$

with

$$\omega_+ = \frac{1}{1+2\gamma_+^2}, \quad \gamma_+ = \frac{\epsilon + (u_{i,j}-2u_{i+1,j}+u_{i+2,j})^2}{\epsilon + (u_{i+1,j}-2u_{i,j}+u_{i-1,j})^2}. \tag{28}$$

Similarly, we can define third-order WENO approximations for $(u_z)^-_{i,j}$ and $(u_z)^+_{i,j}$. ϵ is a small positive number to avoid division by zero.

Thus we have the following Lax–Friedrichs scheme based on the third-order WENO approximations,

$$\begin{aligned} u^{new}_{i,j} = \left(\frac{1}{\alpha_x/h+\alpha_z/h}\right)\Bigg[& f_{i,j} - H\left(x_i, z_j, u^{old}_{i,j}, \frac{(u_x)^-_{i,j}+(u_x)^+_{i,j}}{2}, \frac{(u_z)^-_{i,j}+(u_z)^+_{i,j}}{2}\right) + \alpha_x \frac{2u^{old}_{i,j} + h\left((u_x)^+_{i,j}-(u_x)^-_{i,j}\right)}{2h} \\ & + \alpha_z \frac{2u^{old}_{i,j} + h\left((u_z)^+_{i,j}-(u_z)^-_{i,j}\right)}{2h}\Bigg]. \end{aligned} \tag{29}$$

Here $u^{new}_{i,j}$ denotes the to-be-updated numerical solution for u at the grid point (i,j), and $u^{old}_{i,j}$ denotes the current old value for u at the same point.

The third-order Lax–Friedrichs sweeping method for Eq. (19) is summarized as follows [8,28]:

1. Initialization: assign exact values or interpolate values at grid points within a square region centered at the source point with size equal to $2h \times 2h$, such that the grid points are enough for the third-order WENO approximations. These values are fixed during iterations.
2. Iterations: update $u^{new}_{i,j}$ in (29) by Gauss–Seidel iterations with four alternating directions:

   (1) $i = 1:I$, $j = 1:J$; (2) $i = 1:I$, $j = J:1$,
   (3) $i = I:1$, $j = 1:J$; (4) $i = I:1$, $j = J:1$.

3. Convergence: if

$$\left|u^{new}_{i,j} - u^{old}_{i,j}\right|_\infty \leqslant \delta,$$

where δ is a given convergence threshold value, the iterations converge and the algorithm stops.

We use this scheme to solve the factored equations (without confusion of notations):

- Eq. (11) with Hamiltonian and f as

$$H(x,z,u,u_x,u_z) = \sqrt{\tau_0^2(u_x^2+u_z^2) + 2\tau_0 u(\tau_{0x}u_x + \tau_{0z}u_z) + u^2 s_0^2},$$
$$f = s;$$

Please cite this article in press as: S. Luo, J. Qian, Factored singularities and high-order Lax–Friedrichs sweeping schemes for point-source traveltimes and amplitudes, J. Comput. Phys. (2011), doi:10.1016/j.jcp.2011.02.043

- Eq. (14) with Hamiltonian and f as

$$H(x,z,\phi,\phi_x,\phi_z) = (\tau_{0x}u + \tau_0 u_x)\phi_x + (\tau_{0z}u + \tau_0 u_z)\phi_z + \tau_0(u_x\phi_{0x} + u_z\phi_{0z}),$$
$$f = 0;$$

- Eq. (17) with Hamiltonian and f as

$$H(x,z,c,c_x,c_z) = (\tau_0\tau_{yy0}u_x + u\tau_{yy0}\tau_{0x})c_x + (\tau_0\tau_{yy0}u_z + u\tau_{yy0}\tau_{0z})c_z + \left[\tau_0(\tau_{yy0_x}u_x + \tau_{yy0_z}u_z) - \tau_{yy0}^2 u\right]c + \tau_{yy0}^2 c^2,$$
$$f = 0.$$

5. Numerical examples

In this section, we present several examples to demonstrate the performance of our method. In the following numerical examples, we choose $v_0 = 1$. Therefore, $s_0 = 1$, $\tau_0 = \sqrt{(x-x_0)^2 + (z-z_0)^2}$, and $\phi_0 = \frac{\pi}{2} - \arctan\left(\frac{x-x_0}{z-z_0}\right)$ if $z \geqslant z_0, \phi_0 = \frac{3\pi}{2} - \arctan\left(\frac{x-x_0}{z-z_0}\right)$ otherwise.

5.1. Traveltime and amplitude

To justify our numerical schemes, we first use an example to compare our results with those obtained by the adaptive method in [16]. Then we apply our method to three other velocity models including the smooth Marmousi velocity model.

Example 1. we consider a velocity field given by

$$v(x,z) = \begin{cases} 1.0, & \text{if } z \leqslant 0.18, \\ 1.0 + 0.25(z-0.18)^2 \sin(x+1.1), & \text{else.} \end{cases} \tag{30}$$

The domain is $[-1,1] \times [0,3]$. The source is located at $(0,0)$. The velocity field and the traveltime computed by our method are shown in Fig. 1.

We compare the numerical results obtained by our method with those by the adaptive method in [16]. Since the adaptive method in [16] is so far the only finite-difference method which yields reliable traveltimes and amplitudes in the viscosity sense and is designed according to a different principle to treat the source singularity, we use the adaptive method as an independent tool to calibrate our method. Fig. 2 shows the comparisons for τ_x, τ_z, ϕ_x, ϕ_z, τ_{yy} and 2.5-D amplitude on a 101×151 mesh. From the figure we see that numerical results computed by our method match well with the results obtained by the adaptive method in [16].

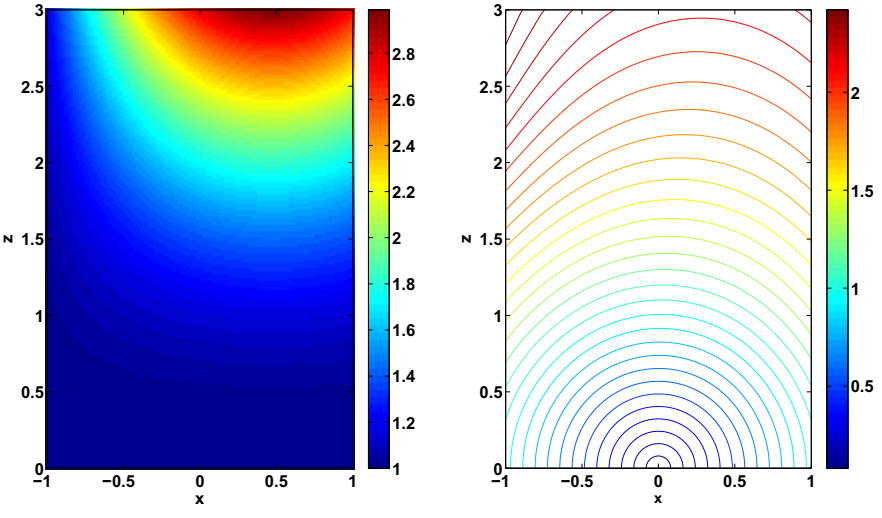

Fig. 1. Example 1. Left: velocity field; right: traveltime with our method.

Please cite this article in press as: S. Luo, J. Qian, Factored singularities and high-order Lax–Friedrichs sweeping schemes for point-source traveltimes and amplitudes, J. Comput. Phys. (2011), doi:10.1016/j.jcp.2011.02.043

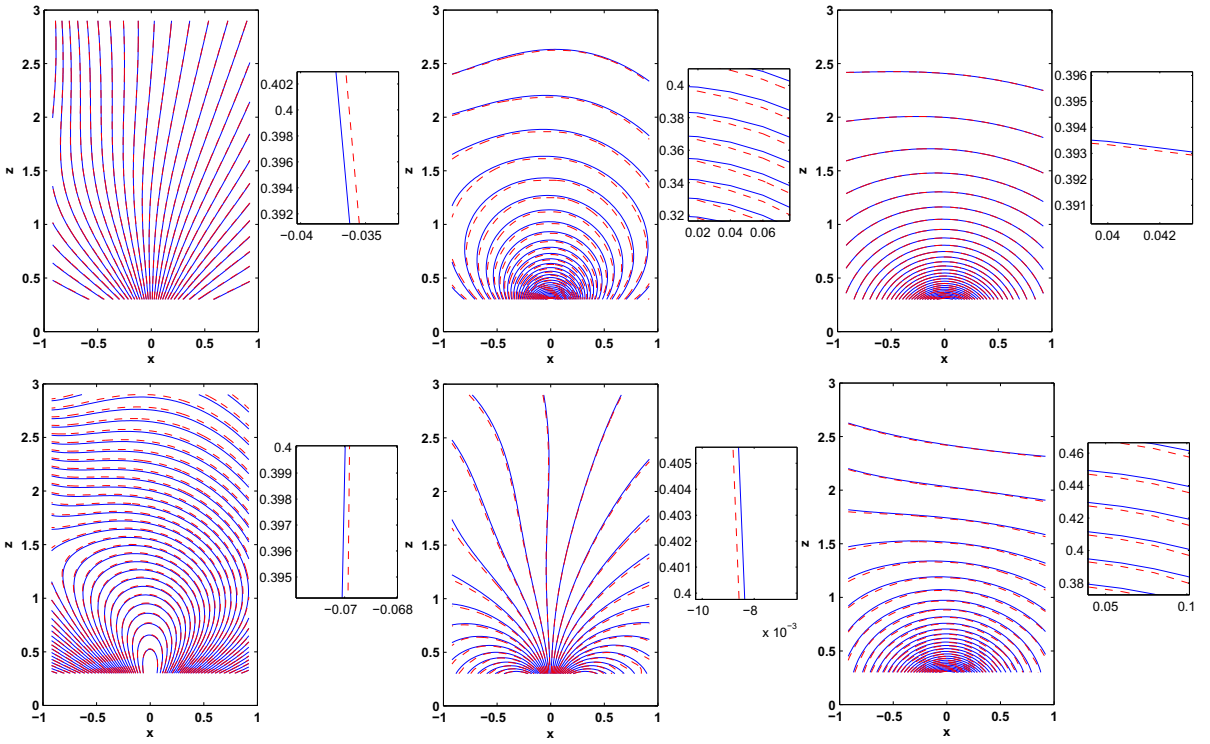

Fig. 2. Example 1. Blue line: our method; red dash line: adaptive method in [16]. Top: τ_x, ϕ_x and τ_{yy}; bottom: τ_z, ϕ_z and 2.5-D amplitude. Zoom-into the window on the right. (For interpretation of the references to colour in this figure legend, the reader is referred to the web version of this article.)

Table 1
Example 2. Maximum error and L_1 error of the traveltime.

Error of traveltime (1.0e−7) on $[0.01, 0.49] \times [-0.24, 0.49]$				
Mesh	51×76	101×151	201×301	401×601
Maximum error	229.09	35.33	1.5155	0.007642
Convergence Order	–	2.7	4.5	7.6
L_1 error	1.163	0.0921	0.003124	0.00021
Convergence Order	–	3.7	4.9	3.9

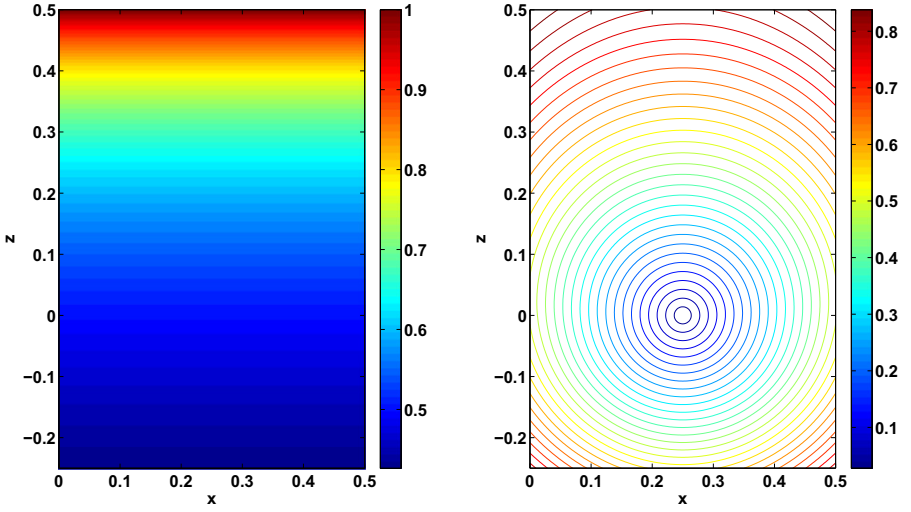

Fig. 3. Example 2. Left: velocity field; right: traveltime with our method.

Please cite this article in press as: S. Luo, J. Qian, Factored singularities and high-order Lax–Friedrichs sweeping schemes for point-source traveltimes and amplitudes, J. Comput. Phys. (2011), doi:10.1016/j.jcp.2011.02.043

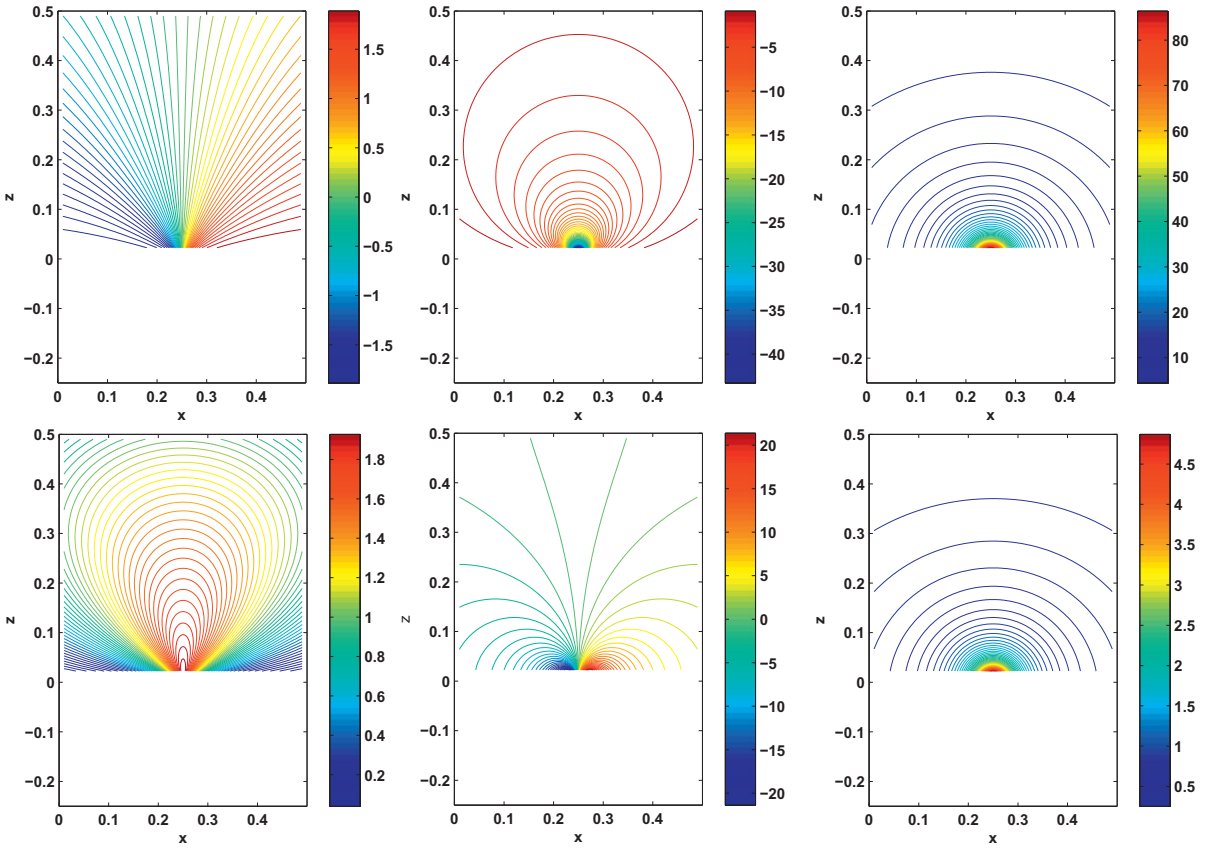

Fig. 4. Example 2. Top: τ_x, ϕ_x and τ_{yy}; bottom: τ_z, ϕ_z and 2.5-D amplitude.

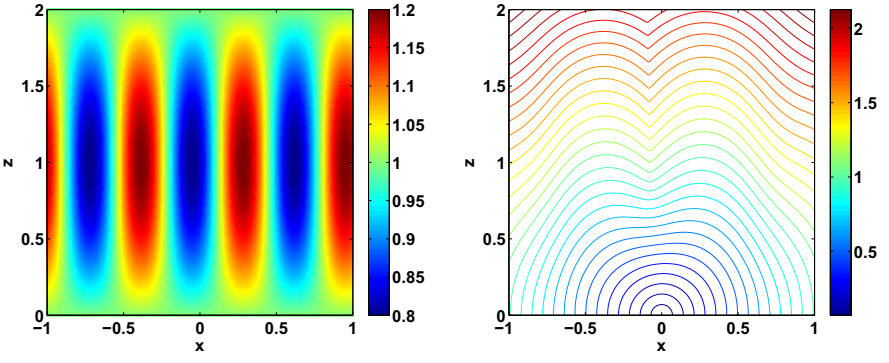

Fig. 5. Example 3. Left: velocity field; right: traveltime with our method.

Example 2. we consider a velocity field in [5] given by

$$v(x,z) = \frac{1}{\sqrt{4.0 + 2.0[g_x(x - x_0) + g_z(z - z_0)]}} \tag{31}$$

with $(g_x, g_z) = (0, -3)$ and the source point $(x_0, z_0) = (0.25, 0)$. In this case, the exact traveltime is known and is smooth. The domain is $[0, 0.5] \times [-0.25, 0.5]$.

Table 1 shows the maximum error and L_1 error (with magnitude 10^{-7}) on $[0.01, 0.49] \times [-0.24, 0.49]$. Fig. 3 shows the velocity field and the traveltime computed by our method. Fig. 4 shows the results for τ_x, τ_z, ϕ_x, ϕ_z, τ_{yy} and 2.5-D amplitude on a 201×301 mesh. For illustration purpose, we only show the contours for $z > 0.025$.

Please cite this article in press as: S. Luo, J. Qian, Factored singularities and high-order Lax–Friedrichs sweeping schemes for point-source traveltimes and amplitudes, J. Comput. Phys. (2011), doi:10.1016/j.jcp.2011.02.043

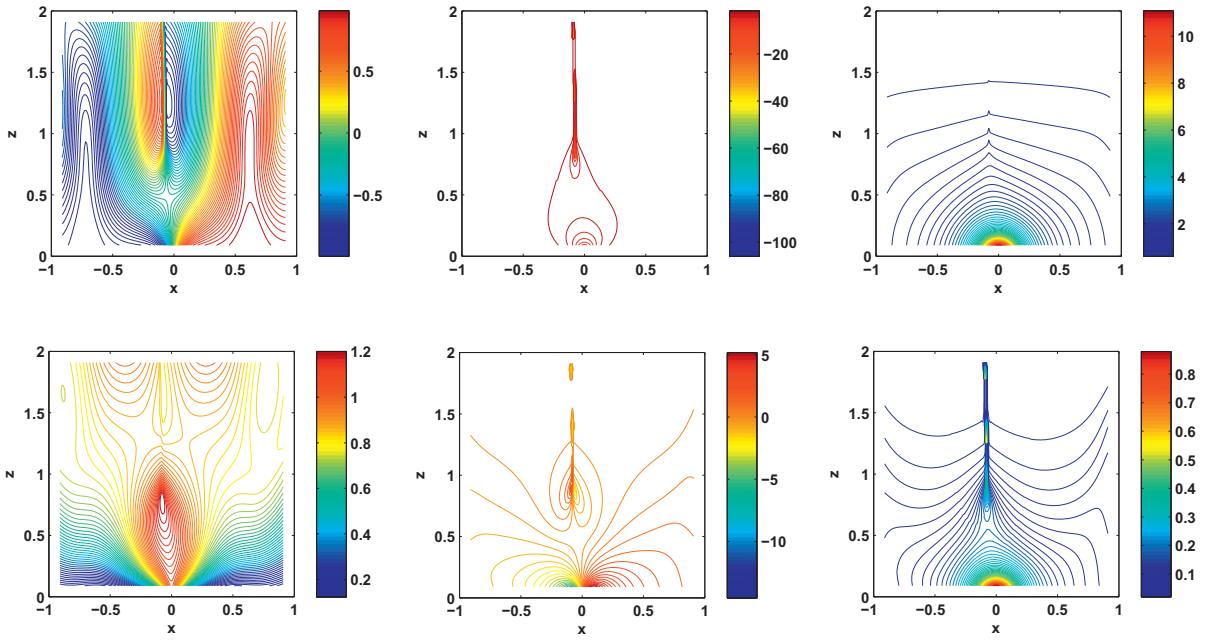

Fig. 6. Example 3. Top: τ_x, ϕ_x and τ_{yy}; bottom: τ_z, ϕ_z and 2.5-D amplitude.

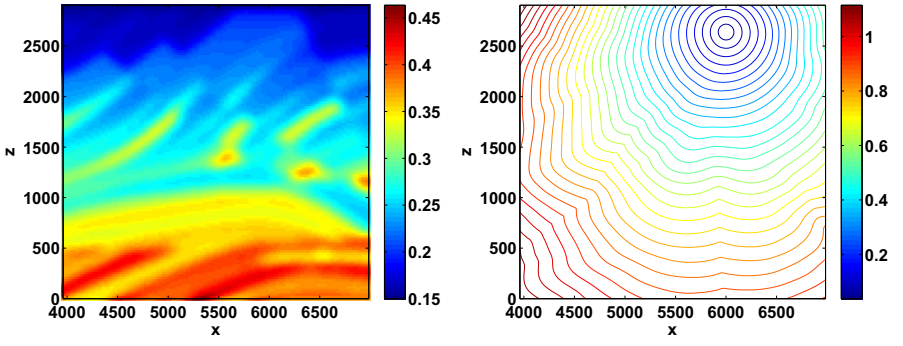

Fig. 7. Example 4. Left: Marmousi velocity field; right: traveltime with our method.

Example 3 (*Sinusoidal model*). the velocity field is given by

$$v(x,z) = 1 + 0.2\sin(0.5\pi z)\sin(3\pi(x+0.55)). \tag{32}$$

The domain is $[-1,1]\times[0,2]$ and the source point is $(0,0)$. Fig. 5 shows the velocity field and the traveltime computed by our method. Fig. 6 shows the results for τ_x, τ_z, ϕ_x, ϕ_z, τ_{yy} and 2.5-D amplitude on a 201×201 mesh.

As is known, in this case the traveltime field is not smooth everywhere away from the source. In fact, the physical traveltime field is multivalued as shown in [15]. However, the high-order Lax–Friedrichs sweeping scheme is based on the monotone scheme which only yields the viscosity-solution based single-valued solution. Consequently, we see kinks in the computed traveltime field as shown in Fig. 5; when numerically differentiated these kinks will produce discontinuities as shown in Fig. 6. Nevertheless, those discontinuities are confined near the kinks because the underlying numerical schemes are essentially upwinding.

Example 4 (*Marmousi velocity model*). we consider the smooth Marmousi velocity model as in Fig. 7. Note that the velocity is rescaled by a factor 10^{-4}. The mesh is 127×122.

The traveltime computed with our method is shown in Fig. 7. Fig. 8 shows the results for τ_x, τ_z, ϕ_x, ϕ_z, τ_{yy} and 2.5-D amplitude. In this case, we also see kinks in computed traveltime field and discontinuities in other computed quantities.

Please cite this article in press as: S. Luo, J. Qian, Factored singularities and high-order Lax–Friedrichs sweeping schemes for point-source traveltimes and amplitudes, J. Comput. Phys. (2011), doi:10.1016/j.jcp.2011.02.043

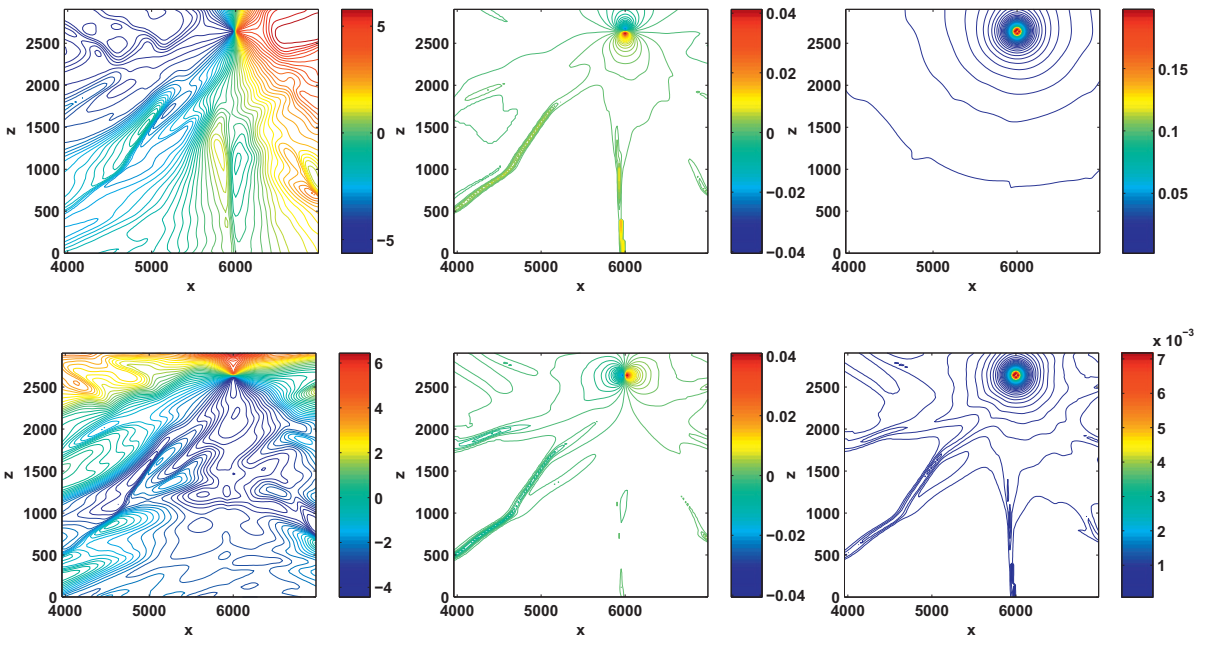

Fig. 8. Example 4. Top: τ_x, ϕ_x and τ_{yy}; bottom: τ_z, ϕ_z and 2.5-D amplitude.

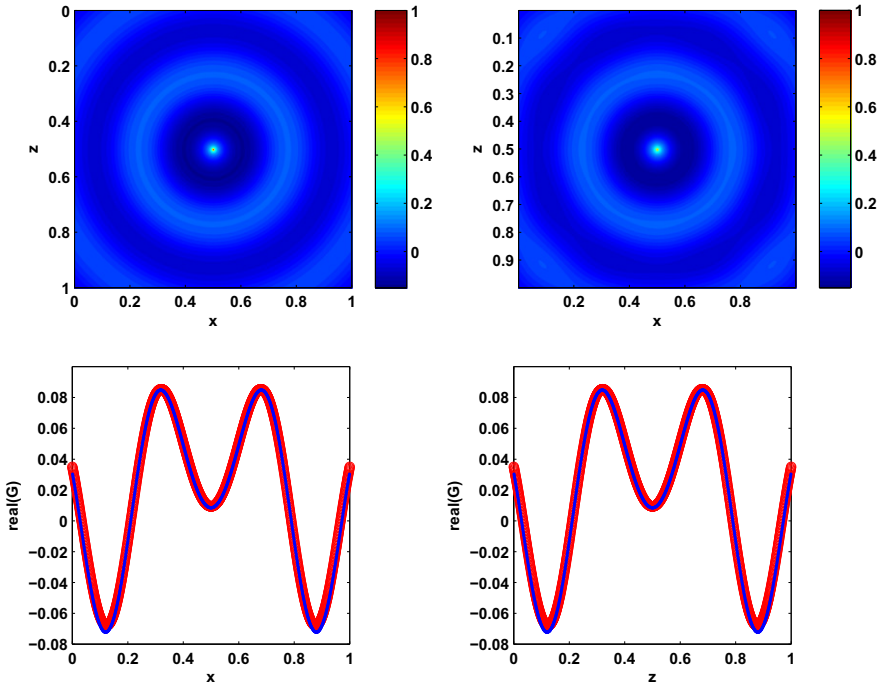

Fig. 9. Example 5.1. Two-dimensional Green function. Top: image of the real part of the Green function (left: our method, right: Helmholtz solver). Bottom: two slices of the Green function (real part) at $x = 0.3$ (left) and $z = 0.3$ (right). Red circle: our method. Blue dot: Helmholtz solver in [4]. $\omega = 32\pi$. (For interpretation of the references to colour in this figure legend, the reader is referred to the web version of this article.)

5.2. Wavefield construction

Now that traveltime and amplitude functions are available, we may construct the asymptotic Green function for the Helmholtz equation in the high frequency regime. However, because computed traveltimes and amplitudes are based on

Please cite this article in press as: S. Luo, J. Qian, Factored singularities and high-order Lax–Friedrichs sweeping schemes for point-source traveltimes and amplitudes, J. Comput. Phys. (2011), doi:10.1016/j.jcp.2011.02.043

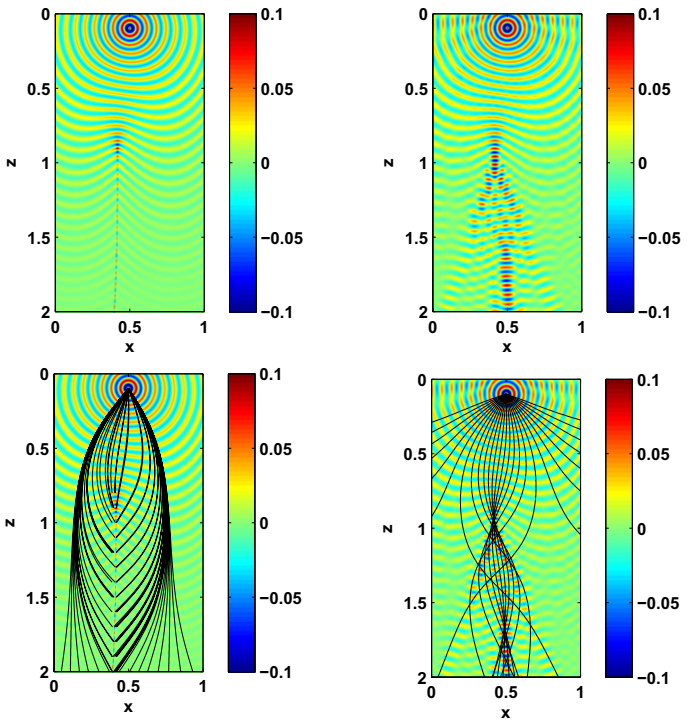

Fig. 10. Example 5.2. Top: two-dimensional Green functions (real part); bottom: Green functions with rays. Left: our method; right: Helmholtz solver in [4]. $\omega = 32\pi$. (For interpretation of the references to colour in this figure legend, the reader is referred to the web version of this article.)

the concept of viscosity solutions, the constructed Green function is an approximation to the true Green function in the weak sense in that the constructed Green function approximates the true Green function faithfully only when the traveltime field is smooth (with no kinks), and the constructed Green function approximates the true Green function unfaithfully when the traveltime field is not smooth with kinks. To demonstrate this feature clearly, we will show a couple of examples.

Example 5 (*Green functions*). we use our results to approximate the Green function for the Helmholtz equation in the high frequency regime,

$$\nabla^2 G(x,z,\omega) + \frac{\omega^2}{v^2(x,z)} G(x,z,\omega) = -\delta(x-x_0)\delta(z-z_0), \tag{33}$$

where $G(x,z,\omega)$ is the Green function, and ω is a given frequency.

We approximate the two-dimensional Green function in the WKBJ form (Appendix C in [11]),

$$G_2(x,z,\omega) \approx \frac{1}{\sqrt{\omega}} A(x,z) e^{i(\omega\tau(x,z)+\frac{\pi}{4})}, \tag{34}$$

where A is given by Eq. (5).

Two velocity models are used to test our results, and we compare the constructed Green functions with those obtained by the direct finite-difference solver of the Helmholtz equation in [4]. We choose $\omega = 32\pi$.

1. $v(x,z) \equiv 5.0$, $(x_0,z_0) = (0.5,0.5)$, domain $[0,1] \times [0,1]$. Fig. 9 shows the results for the two-dimensional Green function on a 1200×1200 mesh. The results by our method are very close to those obtained by the Helmholtz solver.
2. $v(x,z) = 1 + 0.2\sin(0.5\pi z)\sin(3\pi(x+0.05))$, $(x_0,z_0) = (0.5,0.1)$, domain $[0,1] \times [0,2]$. Fig. 10 shows the results for the real part of the two-dimensional Green function on a 800×1600 mesh. Fig. 11 shows two slices at $z = 0.3$ (no kinks, no caustics) and $z = 1.5$ (kinks, caustics).

We remark that numerical errors of a direct solver for the Helmholtz equation depend on the frequency ω as analyzed in the form of pollution errors in [1]. Thus, the direct finite-difference solver for the Helmholtz equation as designed in [4] unavoidably shows polluted errors in the form of large dispersion errors and nonphysical small oscillations as ω becomes large, which are evident in the direct solution shown here. Nevertheless, for ω not so large, the direct solution still provides reasonable results for our comparison purpose.

Please cite this article in press as: S. Luo, J. Qian, Factored singularities and high-order Lax–Friedrichs sweeping schemes for point-source traveltimes and amplitudes, J. Comput. Phys. (2011), doi:10.1016/j.jcp.2011.02.043

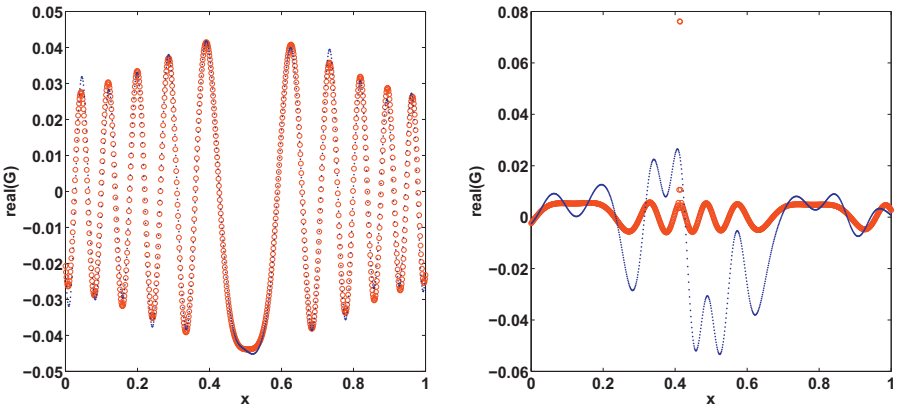

Fig. 11. Example 5.2. Two slices of the two-dimensional Green function at $z = 0.3$ (no kinks, no caustics) and $z = 1.5$ (kinks, caustics). Red circle: our method. Blue dot: Helmholtz solver in [4]. $\omega = 32\pi$. (For interpretation of the references to colour in this figure legend, the reader is referred to the web version of this article.)

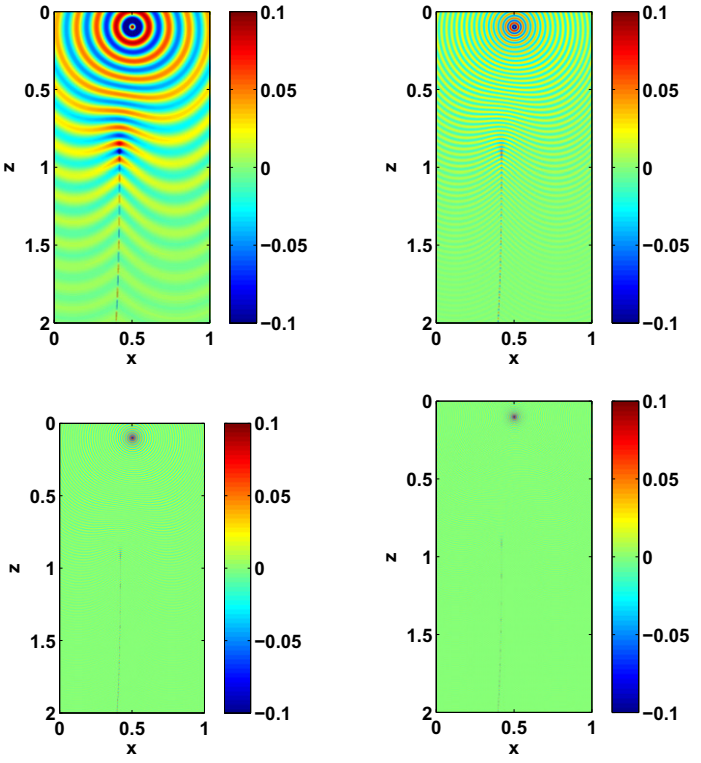

Fig. 12. Example 6. Green functions constructed with our method. Top-left: $\omega = 16\pi$; top-right: $\omega = 64\pi$. Bottom-left: $\omega = 128\pi$; bottom-right: $\omega = 180\pi$. (For interpretation of the references to colour in this figure legend, the reader is referred to the web version of this article.)

Case 1 Because the traveltime field is smooth everywhere away from the source, the constructed asymptotic Green function approximates the true Green function faithfully.

Case 2 Because the traveltime field is not smooth, the constructed Green function in the weak sense cannot approximate the true Green function faithfully as shown in Fig. 10. In fact, the traveltime field in the viscosity-solution sense is single-valued, and the resulting ray structure is shown in the bottom-left subfigure. On the other hand, to reconstruct the true Green function, we need the multivalued traveltime field, and the resulting ray structure is shown in the bottom-right subfigure. Consequently, there is an essential difference between single-valued and multivalued traveltime fields.

Please cite this article in press as: S. Luo, J. Qian, Factored singularities and high-order Lax–Friedrichs sweeping schemes for point-source traveltimes and amplitudes, J. Comput. Phys. (2011), doi:10.1016/j.jcp.2011.02.043

We also mention that before kinks appear in the single-valued traveltime field or caustics appear in the multivalued traveltime field, the true traveltime field is smooth and the asymptotic Green function in the single-valued and multi-valued sense approximates the true Green function faithfully. Only after kinks appear in the single-valued traveltime field or caustics appear in the multivalued traveltime field, the two traveltime fields yield totally different Green functions, as shown clearly in Fig. 11.

Example 6 (*Green functions for different frequencies).* we notice that by the geometrical-optics ansatz the traveltime and amplitude functions are independent of the frequency ω. Thus, computed traveltime and amplitude functions on a certain mesh actually provide ingredients for constructing Green functions in a certain range of frequencies rather than at a single frequency.

As an example, we construct Green functions for $\omega = 16\pi$, $\omega = 64\pi$, $\omega = 128\pi$, and $\omega = 180\pi$ in the case of the sinusoidal model given in Example 5. We remark that when $\omega = 180\pi$, the finite-difference direct solver, such as the direct Helmholtz solver in [4], requires too many grid points, which is no longer efficient. However, our method does not suffer from such a grid dependence. Fig. 12 shows the constructed Green functions with $\omega = 16\pi$, $\omega = 64\pi$, $\omega = 128\pi$, and $\omega = 180\pi$ based on traveltimes and amplitudes computed by our method on a 800×1600 mesh.

6. Conclusions

We present a factorization technique based on the factored Eikonal equation to compute the takeoff angle and the out-of-plane curvature, thus the amplitude. We decompose the takeoff angle and the out-of plane curvature into two additive and multiplicative factors, respectively. One of them is known analytically corresponding to a constant velocity field, and it captures the local properties of the takeoff angle or the out-of-plane curvature well in the neighborhood of the source. Then a third-order WENO based Lax–Friedrichs sweeping method is applied to solve the factored equations numerically. The advantage of decomposing the takeoff angle into two additive factors is that since the known factor captures the local properties such as the angular directions of the takeoff angle at the source, the other factor can be initialized easily at the source. The advantage of decomposing the out-of-plane curvature into two multiplicative factors is that since the known factor captures the source singularity, the other factor is smooth at the source. Numerical examples are presented to demonstrate the performance of our new method.

Acknowledgment

Qian would like to dedicate this paper to Professor Jiaqi Liu of Harbin Institute of Technology on the occasion of his 70th birthday.

References

[1] I.M. Babuška, S.A. Sauter, Is the pollution effect of the FEM avoidable for the Helmholtz equation considering high wave numbers?, SIAM Rev 42 (2000) 451–484.
[2] V. Cerveny, I.A. Molotkov, I. Psencik, Ray Method in Seismology, Univ. Karlova Press, 1977.
[3] M.G. Crandall, P.-L. Lions, Viscosity solutions of Hamilton–Jacobi equations, Trans. Amer. Math. Soc. 277 (1983) 1–42.
[4] Y.A. Erlangga, C.W. Oosterlee, C. Vuik, A novel multigrid-based preconditioner for the heterogeneous Helmholtz equation, SIAM J. Sci. Comput. 27 (2006) 1471–1492.
[5] S. Fomel, S. Luo, H.-K. Zhao, Fast sweeping method for the factored Eikonal equation, J. Comput. Phys. 228 (17) (2009) 6440–6455.
[6] F. Friedlander, Sound Pulses, Cambridge Univ. Press, 1958.
[7] C. Kao, S. Osher, J. Qian, Legendre transform based fast sweeping methods for static Hamilton–Jacobi equations on triangulated meshes, J. Comput. Phys. 227 (2008) 10209–10225.
[8] C.Y. Kao, S. Osher, J. Qian, Lax–Friedrichs sweeping schemes for static Hamilton–Jacobi equations, J. Comput. Phys. 196 (2004) 367–391.
[9] C.Y. Kao, S.J. Osher, Y.-H. Tsai, Fast sweeping method for static Hamilton–Jacobi equations, SIAM J. Numer. Anal. 42 (2005) 2612–2632.
[10] S. Kim, R. Cook, 3D traveltime computation using second-order ENO scheme, Geophysics 64 (1999) 1867–1876.
[11] S. Leung, J. Qian, R. Burridge, Eulerian–Gaussian beams for high-frequency wave propagation, Geophysics 72 (5) (2007) SM61–SM76.
[12] F. Li, C.-W. Shu, Y.-T. Zhang, H.-K. Zhao, A second-order discontinuous Galerkin fast sweeping method for Eikonal equations, J. Comput. Phys. 227 (2008) 8191–8208.
[13] P.-L. Lions, Generalized Solutions of Hamilton–Jacobi Equations, Pitman, Boston, 1982.
[14] S. Osher, C.-W. Shu, High-order essentially nonoscillatory schemes for Hamilton–Jacobi equations, SIAM J. Math. Anal. 28 (4) (1991) 907–922.
[15] J. Qian, S. Leung, A level set method for paraxial multivalued traveltimes, J. Comput. Phys. 197 (2004) 711–736.
[16] J. Qian, W.W. Symes, An adaptive finite-difference method for traveltimes and amplitudes, Geophysics 67 (2002) 167–176.
[17] J. Qian, Y.T. Zhang, H.K. Zhao, Fast sweeping methods for Eikonal equations on triangulated meshes, SIAM J. Numer. Anal. 45 (2007) 83–107.
[18] J. Qian, Y.T. Zhang, H.K. Zhao, Fast sweeping methods for static Hamilton–Jacobi equations on triangulated meshes, J. Sci. Comput. 31 (2007) 237–271.
[19] F. Qin, Y. Luo, K.B. Olsen, W. Cai, G.T. Schuster, Finite difference solution of the Eikonal equation along expanding wavefronts, Geophysics 57 (1992) 478–487.
[20] W.A. Schneider Jr., Robust and efficient upwind finite-difference traveltime calculations in three dimensions, Geophysics 60 (1995) 1108–1117.
[21] S. Serna, J. Qian, A stopping criterion for higher-order sweeping schemes for static Hamilton–Jacobi equations, J. Comput. Math. 28 (2010) 552–568.
[22] J.A. Sethian, Level Set Methods and Fast Marching Methods: Evolving Interfaces in Computational Geometry, Fluid Mechanics, Computer Vision, and Materials Science, Cambridge University Press, 1999.
[23] J.A. Sethian, A.M. Popovici, 3-D traveltime computation using the fast marching method, Geophysics 64 (2) (1999) 516–523.
[24] W.W. Symes, R. Versteeg, A. Sei, Q.H. Tran, Kirchhoff simulation migration and inversion using finite-difference travel-times and amplitudes, TRIP Technical Report, Rice U., 1994.
[25] R. Tsai, L.-T. Cheng, S.J. Osher, H.K. Zhao, Fast sweeping method for a class of Hamilton–Jacobi equations, SIAM J. Numer. Anal. 41 (2003) 673–694.

Please cite this article in press as: S. Luo, J. Qian, Factored singularities and high-order Lax–Friedrichs sweeping schemes for point-source traveltimes and amplitudes, J. Comput. Phys. (2011), doi:10.1016/j.jcp.2011.02.043

[26] J. van Trier, W.W. Symes, Upwind finite-difference calculation of traveltimes, Geophysics 56 (06) (1991) 812–821.
[27] J.E. Vidale, Finite-difference calculation of traveltimes in three dimensions, Geophysics 55 (05) (1990) 521–526.
[28] Y.-T. Zhang, H.-K. Zhao, J. Qian, High order fast sweeping methods for static Hamilton–Jacobi equations, J. Sci. Comput. 29 (2006) 25–56.
[29] H.-K. Zhao, A fast sweeping method for Eikonal equations, Math. Comput. 74 (2005) 603–627.

Please cite this article in press as: S. Luo, J. Qian, Factored singularities and high-order Lax–Friedrichs sweeping schemes for point-source traveltimes and amplitudes, J. Comput. Phys. (2011), doi:10.1016/j.jcp.2011.02.043